Title
Closing yield gap is crucial to avoid potential surge in global carbon emissions

Authors
Suh, Sangwon
Johnson, Justin A
Tambjerg, Lau
et al.

Publication Date
2020-07-01

DOI
10.1016/j.gloenvcha.2020.102100

Peer reviewed

Abstract

Global greenhouse gas (GHG) emissions models generally project a downward trend in CO_2 emissions from land use change, assuming significant crop yield improvements. For some crops, however, significant yield gaps persist whilst demand continues to rise. Here we examine the land use change and GHG implications of meeting growing demand for maize. Integrating economic and biophysical models at an unprecedented spatial resolution, we show that CO_2 emissions from land conversion may rise sharply if future yield growth follows historical trends. Our results show that ~4.0 Gt of additional CO_2 would be emitted from ~23 Mha agricultural expansion from 2015 to 2026, under historical yield improvement trends. If yield gaps are closed expeditiously, however, GHG emissions can be reduced to ~1.1 Gt CO_2 during the period. Our results highlight the urgent need to close global yield gaps to minimize agricultural expansion and for continued efforts to constrain agricultural expansion in carbon-rich lands and forests.

1. Introduction

Agriculture already occupies about 40% of global land and yet global food demand is expected to increase by 60-110% by 2050[1,2]. Natural land conversion to cropland has been the largest source of land-based CO_2 emissions in the last century[3]. However, CO_2 emissions from land conversion have been slowing down from the turn of this century following the trends in yield increase and the declining rate of deforestation in recent decades[4]. Reflecting these trends, the baseline scenarios of the Fifth Assessment Report by the Intergovernmental Panel for Climate Change (IPCC) project CO_2 emissions from agricultural expansion approaching zero by around 2070[4]. Similarly, an ensemble of 18 Integrated Assessment Models (IAMs) also project a declining trend in CO_2 emissions from land use change, the range of which will eventually reach near or below zero annual emissions by 2100 for all three scenarios evaluated including baseline, 550ppm, and 450ppm scenarios[5]. While the Shared Socio-economic Pathways (SSPs) on land-use futures present a wide range of possible emission scenarios from ~750 Gt CO_2 yr^{-1} reduction (SSP1, RCP 2.6) to 400 Gt CO_2 yr^{-1} increase (SSP3, baseline) from agricultural land use change by 2100[6], the baseline scenario generally projects declining CO_2 emissions from land use change and continued yield improvement around the globe for the second half of the century[6].[1]

While CO_2 emissions from land conversion are widely expected to diminish, greenhouse gas (GHG) emissions from land use management, mainly CH_4 and N_2O, are expected to increase throughout this century[4,5,7,8].

[1] Notable exceptions are SSP3 (*A rocky road*) and SSP4 (*A road divided*). SSP3 is characterized by limited regulation, continued deforestation, low technological development and resource-intensive consumption. SSP4 is characterized by a division between high to medium income countries (and consumers) and low-income countries (and consumers), where only high to medium income countries (and consumers) are exposed to tougher regulations and efficient technologies.

These projections typically assume that global crop yield will continue to improve. However, some studies have observed a stagnation in yield improvement trends; large yield gap persists in some regions, which call the prevailing projections of declining land use change and associated emissions into question[9,10].

In this study, we develop a high-resolution spatial model with multiple yield improvement scenarios to examine the implications of global yield improvement trajectories on GHG emissions from future maize production. More than half of current agricultural land is used for cereal production[2,11], and maize is the largest agricultural crop in terms of production volume, fulfilling about 40% of global grain needs[12]. Global maize consumption has more than doubled since 1990, at an annual growth rate of ~3%; biofuel and feed were the main drivers of this growth in recent years[13]. However, the total cultivated land area for maize has remained stable due to the remarkable increase in global average yield; between 1980 and 2010, global average maize yield increased by ~50% from 3.4 t ha^{-1} to 5.1 t ha^{-1} (5 year moving average)[2]. Average maize yield in Asia has doubled during the 30 year period, whereas that in Africa increased only 28%[2]. Technological changes including the use of irrigation, introduction of new crop varieties, fertilizer and agrochemical use, improved management techniques and mechanical equipment have been widely recognized as the drivers of the yield improvements[14–16]. In addition, non-technical factors such as changes in precipitation, temperature and the length of growing seasons have also been identified as contributors to increasing yield trends[15,17]. Nevertheless, future trajectories of global yield improvement are inherently uncertain.

In this study, we employ three maize yield improvement scenarios. Under each scenario, we model the spatial patterns of potential intensification and expansion for the period 2015 – 2026 at 5 by 5 arc-minute resolution covering the globe. We then estimate GHG emissions from land use change and the use of nitrogen fertilizers under each scenario.

2. Methods

2. 1 Scenarios for global yield gap closure

According to OECD-FAO projections and historical data[18], global maize demand amounted to about 1,010 Mt as of 2015; this is expected to grow to 1,186 Mt by 2026. We employ three yield improvement scenarios to describe the potential land use change outcomes to meet 176 Mt additional maize demand between 2015 and 2026.

- **Scenario 1 (baseline)**: historical yield trend scenario, which follows the global yield trends at 5 by 5 arc-minute resolution between 1961 and 2008[9,10] or the average yield improvement between 2000 and 2010, whichever is higher. Yield increases linearly without compounding and stops when it reaches maximum potential yield of the grid-cell. This scenario includes yield stagnation in some regions based on historical data.

- **Scenario 2 (moderate acceleration in yield gap closure)**: yield increases in such a way that up to 5% of the previous year's yield gap is closed per year (depending on the input levels selected). Yield gap is estimated as the difference between the baseline yield (2010) and the maximum potential yield of the grid-cell, using FAOSTAT[2] and Earthstat database[19] (see SI section 1.1.1 for details).
- **Scenario 3 (aggressive acceleration in yield gap closure)**: yield increases in such a way that up to 10% of the previous year's yield gap is closed per year (depending on the input levels selected).

Within the yield gap closure conditions for Scenarios 2 and 3, actual yield (up to the 5 or 10% per year limit) is determined among four yield levels corresponding to no, low, medium, and high input levels. These levels are selected based on whichever one offers the lowest marginal cost of production (Fig. 1). As the remaining yield gap is calculated each year, the same percent of yield gap progressively leads to diminishing yield increases as the yield of a grid-cell improves (see also SI section 1.1 for details).

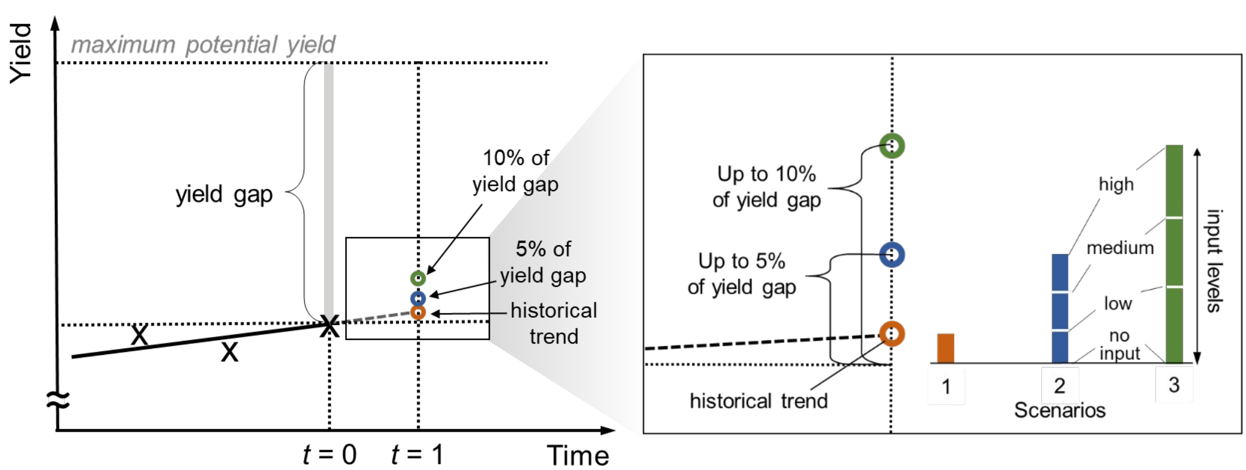

Fig. 1. Yield choices for each grid-cell in year *t* = 1. Under Scenario 1, the yield of a grid-cell is determined following the historical yield trend of the grid-cell. Under Scenarios 2 and 3, the most economic input level determines the yield within the limit set by each scenario (5% and 10% of the remaining yield gap of the previous year for Scenario 2 and Scenario 3, respectively).

2.2 Spatial patterns of agricultural expansion

Spatial patterns of agricultural expansion are known to be critical in determining carbon emissions[20]; however, understanding spatial distribution of future crop production is hampered by the complexity of global land use change dynamics that involve social, climatic, economic, and logistic constraints. Various models have been utilized in the literature to address these challenges including LUCI-LCA[21], GLOBIOM[22,23], GCAM[24], and MAgPIE[25,26]. Assumptions, geographical coverage, spatial resolution, and underlying data and mechanisms employed vary significantly among these models. LUCI-LCA, for example, uses a logistic regression assuming agricultural expansion would take place in areas that resemble the conditions of existing cropland[21]. GLOBIOM and GCAM employ spatially-explicit partial equilibrium models distinguishing 14 – 18 global regions at 30 by 30 arc minute resolution for simulation[22–24], and MAgPIE uses a dynamic vegetation model with a cost minimization function at 30 by 30 arc minute resolution[25,26]. These models either ignore potential spillover effects or use coarse spatial resolutions for yield and carbon stock estimations though they are known to vary widely within hundreds of meters [27,28]. Furthermore, yield responses to inputs are often assumed to be unconstrained, which may result in unrealistically optimistic yield improvements[23].

Our approach is designed to enhance the spatial resolution of land use change projections and to tie future yield improvements to historical data. It accounts for the constraints and decision-making processes operating at these different scales whilst minimizing conceptual and computational challenges such as aggregation and run times. We accomplish this by combining three modeling steps designed to utilize economic, production, infrastructure and biophysical data available at different spatial scales. (1) Global Land Use Change (GLUC) modeling is a spatial extension of the Technology Choice Model (TCM)[29–31] and captures crop production through intensification and expansion based on marginal supply cost curves at a 5 by 5 arc minute—about 10 by 10 km at the equator—resolution. (2) The Spatial Economic Allocation Landscape Simulator (SEALS) refines the GLUC results into 10 by 10 arc second—about 300 by 300 m at the equator—resolution based on adjacency and configuration of different land-use, land-cover (LULC) types and physical suitability using a digital elevation model (DEM) and soil organic carbon (SOC) data. And finally (3) calculation of GHG emissions is performed using a combination of spatially explicit data and models to estimate above ground biomass loss from agricultural expansion for maize, combined with estimates of N_2O emissions from fertilizer use in production intensification.

2.3 Modeling strategy

Our goal is not to predict accurately where agricultural expansion for future marginal maize production will occur, but rather to understand how different future scenarios might affect the landscape. Thus, the maps produced here should not be taken as predictions but rather as useful and detailed hypotheticals that let us assess landscape-level ecosystem service impacts of projected future demand, such as changes in carbon storage.

2.3.1 GLUC model

GLUC is a spatial extension of the Technology Choice Model (TCM) [31] that finds the optimal spatial distribution of crop production at a 5 by 5 arc-minute resolution (2,160×4,320 grid-cells) covering the globe. It is a constrained optimization model that minimizes the global marginal cost of production and transportation needed to meet a given demand.

For each grid-cell that participates in maize production in *t* - 1, the most economical input level at year *t* is chosen among the four options shown in Fig. 1. The corresponding yield is used to calculate the marginal cost of intensification for grid-cells under Scenarios 2 and 3, considering the costs of fertilizer, irrigation, pesticides, and labor (see SI sections 1.1.3 – 1.1.6). For agricultural expansion, initial yield is determined by the yield of the nearest maize producing grid-cell, after applying a 35.5% yield penalty for newly converted lands (see SI section 1.2.1 for details). The marginal cost of expansion for newly converted grid-cells accounts for yield, corresponding input levels, fixed capital cost, land and land conversion costs. (see SI section 1.2 for details). Finally, the cost of transportation from each grid-cell to the nearest city with at least 50,000 inhabitants is added to the grid-cell level marginal costs of intensification and expansion, providing the total marginal cost matrix at 5 by 5 arc-minute resolution (c_{ik} in equation 1).

GLUC assumes that marginal increases in demand for a crop are fulfilled progressively by the least marginal cost producers, which are represented by the grid-cells, within their capacity limits until they collectively satisfy the total marginal demand for the crop in question[31]. The model was run annually from 2010 to 2015, and the resulting production values by country were compared with the historical production data. Based on the comparison, the model is calibrated so that the discrepancy between the model output and FAO production data are minimized. The calibration step is designed to account for intangible costs (and incentives) that are not reflected in the costs of inputs modeled in our study. For example, limited quota for agricultural land use, transaction costs, moratorium or restrictions in land use change, humanitarian aid, and subsidies may not show up in a balance sheet, while imposing practical barriers to production. In order to account for intangible costs, year-over-year production results based only on tangible costs are aggregated per country and compared with FAO's production data[2]. By setting the amount of intangible cost (or incentive) per tonne of maize production as a variable for each country, we calibrated the model so that GLUC production results per country match FAO data for the years 2010 to 2015. The intangible cost (or incentive) by country for the last calibration year (2014 – 2015) is then used for projection years (2015 – 2026).

For the current study, GLUC is configured to estimate annual changes in intensification and expansion production from 2015 to 2026 in response to an increase in demand by solving the following:

$$\min z = \sum_{i,k} c_{ik} x_{ik}$$
$$s.t. \sum_{i,k} x_{ik} \leq d \qquad (1)$$
$$0 \leq x_{ik} \leq m_{ik},$$

where z is the total marginal cost for additional crop production and transportation ($),

d is the total marginal demand for the crop in question (t),

k indicates the method of marginal production (intensification = 1, expansion = 2),

c_{ik} is the marginal cost of producing and transporting 1 tonne of the crop in the grid-cell i ($/t),

x_{ik} is the marginal production of the crop in the grid-cell i (t), and

m_{ik} is the economical maximum marginal production for the grid-cell i (t).

The solution of this optimization problem shows the marginal production through intensification and expansion, and associated costs at 5 by 5 arc-minute resolution (see SI section 1).

The marginal cost c_{ik} is calculated as the sum of all marginal costs such that:

$$c_{ik} = \sum_j c_{ijk} = \sum_j p_{ij} a_{ijk} \qquad (2)$$

where j is the marginal factor for inputs such as water, fertilizer, land, labor, and transportation,

c_{ijk} is the marginal cost of factor input j under the method of marginal production method k in the grid-cell i needed for 1 tonne of crop ($/t),

p_{ij} is the price of input j in the grid-cell i, and

a_{ijk} is the amount of marginal input j in grid-cell i under the production method k.

For the further details on method and the data used, see SI section 1.

2.3.2 SEALS model

The SEALS model spatially allocates the amount of maize expansion given by GLUC to specific grid-cells at the higher resolution (see SI section 2 for details). SEALS uses a land-use, land-cover (LULC) map, that defines the starting condition of the high-resolution landscape, from the European Space Agency's Climate Change Initiative (ESA-CCI) for the year 2015[32]. The suitability of each fine-resolution grid-cell for agricultural expansion for maize is defined based on nearby LULC types (described below as adjacency relationships), physical suitability and constraints on cultivation in order to allocate the change from the coarse projections to the most suitable cells.

In this application, we pare down the 37 ESA-CCI classes to 8 functional types, namely Cropland, Mosaic cropland, Forest, Shrubland, Grassland, Urban, Bare and Water. Then, we create a set of maps that describe the strength of the spatial adjacency effect for each functional type on agricultural expansion for maize (see SI section 2).

To account for physical suitability, we combine information from a digital elevation model (DEM) and soil organic carbon (SOC) data from Hengl et al (2017)[33]. We then apply constraints on cultivation so that no expansion can occur if > 95% of the grid-cell is existing agriculture or if the grid-cell is water or developed land. Finally, we combine adjacency effect, physical suitability and conversion eligibility maps into overall suitability. We then rank this map and iteratively assign expansion to the highest valued grid-cell until each GLUC-resolution grid-cell has all expansion allocated. The output of the SEALS model is used to calculate GHG emissions from agricultural expansion.

2.3.3 GHG emissions

We find globally explicit aboveground carbon loss by calculating the difference between the carbon stock of the baseline LULC map of year 2015, and the map of the predicted scenario. We focus on above ground carbon, as we do not have spatially explicit data available for belowground carbon.

The carbon stocks are computed by identifying an aboveground biomass value based on the land cover class for each of the grid cells within the baseline ESA LULC map[34] and the future LULC map created by SEALS (see SSI section 3).

For the aboveground biomass stock, we use a combination of data sources: 1) For tropical forest, we use the InVEST (v. 3.4) carbon edge effect model[28], which enables consideration of the biomass impact on converted and nearby grid-cells. 2) For non-tropical forest we use the global forest aboveground biomass map developed by Santoro et al. 2018[35], as this provides spatially explicit biomass stock values for the most recent time period of 2010. 3) Finally, for all other natural land cover types we use the IPCC Tier 1 approach[36] as implemented by Ruesch and Gibbs[37]; this provides a globally consistent approach for the remaining land cover types (e.g. shrubs or grassland).

Nitrous oxide (N_2O) emissions from nitrogen fertilizer application are calculated at a 5 by 5 arc minute resolution using the IPCC guidelines[38] (see SI section 3).

3. Results

3. 1 Carbon emissions from agricultural expansion

Our results show that the 176 Mt increase in maize demand predicted between 2015 and 2026 would require ~23 Mha of agricultural expansion and would result in ~4.0 Gt of additional CO_2 assuming historical yield improvement trends at 5 by 5 arc minute resolution. Including N_2O emissions for intensification, the total GHG emissions become ~4.2 Gt CO_2e. Under an aggressive yield improvement scenario, however, agricultural expansion for maize and corresponding CO_2 emissions can be contained within ~5.1 Mha and ~1.1 Gt CO_2, respectively, or ~1.7 Gt CO_2e when accounting for N_2O emissions from fertilizer use.

Under the historical yield trend case (Scenario 1), as much as 45% of marginal maize demand between 2015 and 2026 was met by agricultural expansion (Fig. 2a). Under the moderate yield improvement case (Scenario 2), however, only 25% of the total marginal demand during the period required agricultural expansion (Fig. 2b), which is further reduced to 10% under the aggressive yield improvement case (Scenario 3) (Fig. 2c).

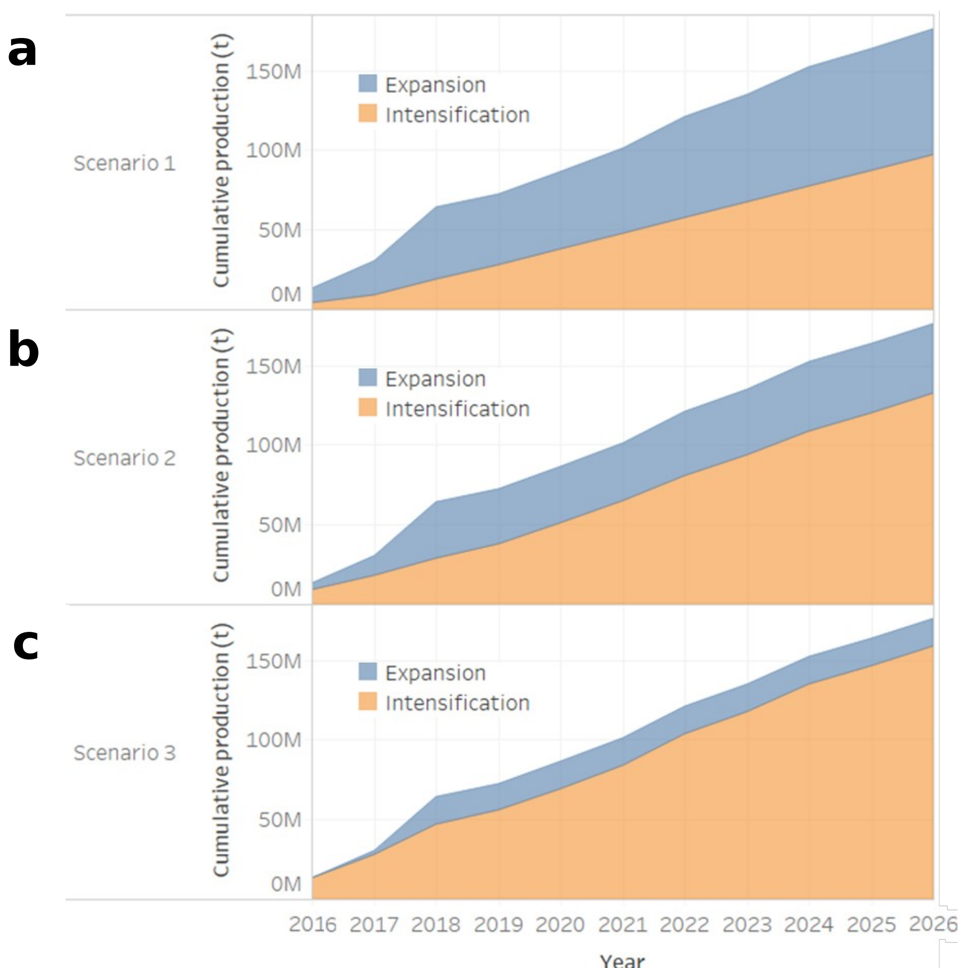

Fig. 2. Simulated marginal production of maize through intensification and expansion between 2015 and 2026 under three yield improvement scenarios (cumulative). (a) Scenario 1: yield improvement following historical trends; (b) Scenario 2: up to 5% additional yield improvement; (c) Scenario 3: up to 10% additional yield improvement

Although it is generally cheaper, intensification alone could not fulfill the marginal demand due to the yield improvement capacity constraints, requiring the system to move on to the more expensive option of agricultural expansion (Fig. 3). Africa, for example, did not contribute signficantly to marginal production via intensification under the historical yield trend scenario despite the presence of large yield gaps (Scenario 1; Fig. 3a). As our model is calibrated using historical production data, on the one hand, the contributions through intensification from the regions with large yield gaps but with limited actual yield improvements, such as Africa and South America, are limited in our model outputs. On the other hand, North America’s marginal production through intensification is estimated to be significant despite the already high yields, given the sustained increase in historical maize production in the region that is reflected in the calibration step (see Section 2.1). Asia and Europe were estimated to absorb a substantial volume of maize demand through expansion. Progress toward closing these yield gaps under Scenarios 2 and 3, however, would allow

Africa and Asia to substantially increase their production through intensification, shrinking agricultural expansion (Fig. 3b and 3c).

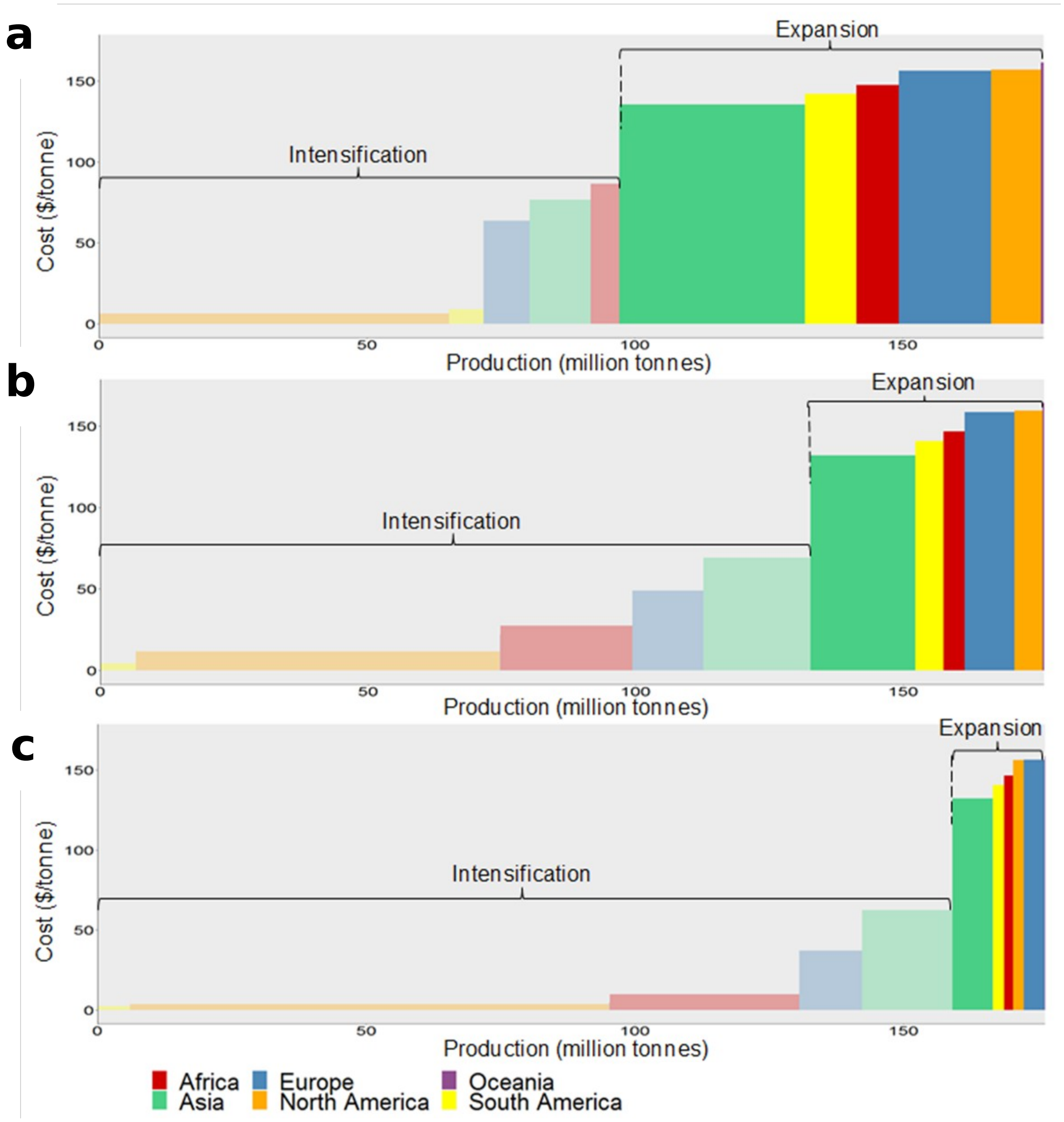

Fig. 3. Marginal supply cost curve of maize through intensification and expansion aggregated at continental level. (a) Scenario 1: yield improvement following historical trends; (b) Scenario 2: up to 5% additional yield improvement; (c) Scenario 3: up to 10% additional

yield improvement. Each block represents production-weighted average marginal supply cost of each region. The marginal costs at 5 by 5 arc-minute resolution within each continent may be significantly higher or lower.

3.2 Regional spatial patterns of expansion

The results of our spatial allocation of agricultural expansion for maize are demonstrated in Fig. 4 for Minnesota, USA. The expansion for maize predicted by GLUC is shown in Fig. 4c and Fig. 4d (in orange). The SEALS model estimates the most likely locations of agricultural expansion within the orange pixels (Fig. 4d; in purple) based on expansion suitability (Fig. 4a) as a function of climate, soil, and slope. The spatial resolution of the remotely-sensed aboveground biomass data shown in Fig. 4b and 4d (in green) matches well with that of the SEALS results (Fig. 4d). Large spatial variance of the aboveground biomass stock of the natural land exists within each GLUC cell **(**Fig. 4b). We find the average carbon stock globally across all GLUC cells where expansion happens to be 31.3 tC ha^{-1} with an average minimum and an average maximum carbon stock of 0.5 and 208.5 tC ha^{-1} respectively. In addition, if no spatially explicit data were used and only the IPCC's tier 1 approach was used at the resolution of GLUC, the CO_2 emissions from agricultural expansion under historical yield trends would be overestimated by 0.3, 0.1 and 0.2 Mt CO_2 in Africa, Asia and South America respectively, and underestimated by 0.7 Mt CO_2 in Europe.

These results illustrate the importance of explictly modeling different phenomena operating at different scales, facilitated here by our multi-step approach. For example, as shown in Fig. 4a, the land in northern Minnesota is highly suitable for maize expansion; this suitability is captured in our finer scale SEALS model. However, economic factors such as infrastructure, capital investment or market access, which operate at regional or national scales and are captured by our coarser-scale GLUC model, are relatively unfavourable for this region (Fig. 4c).

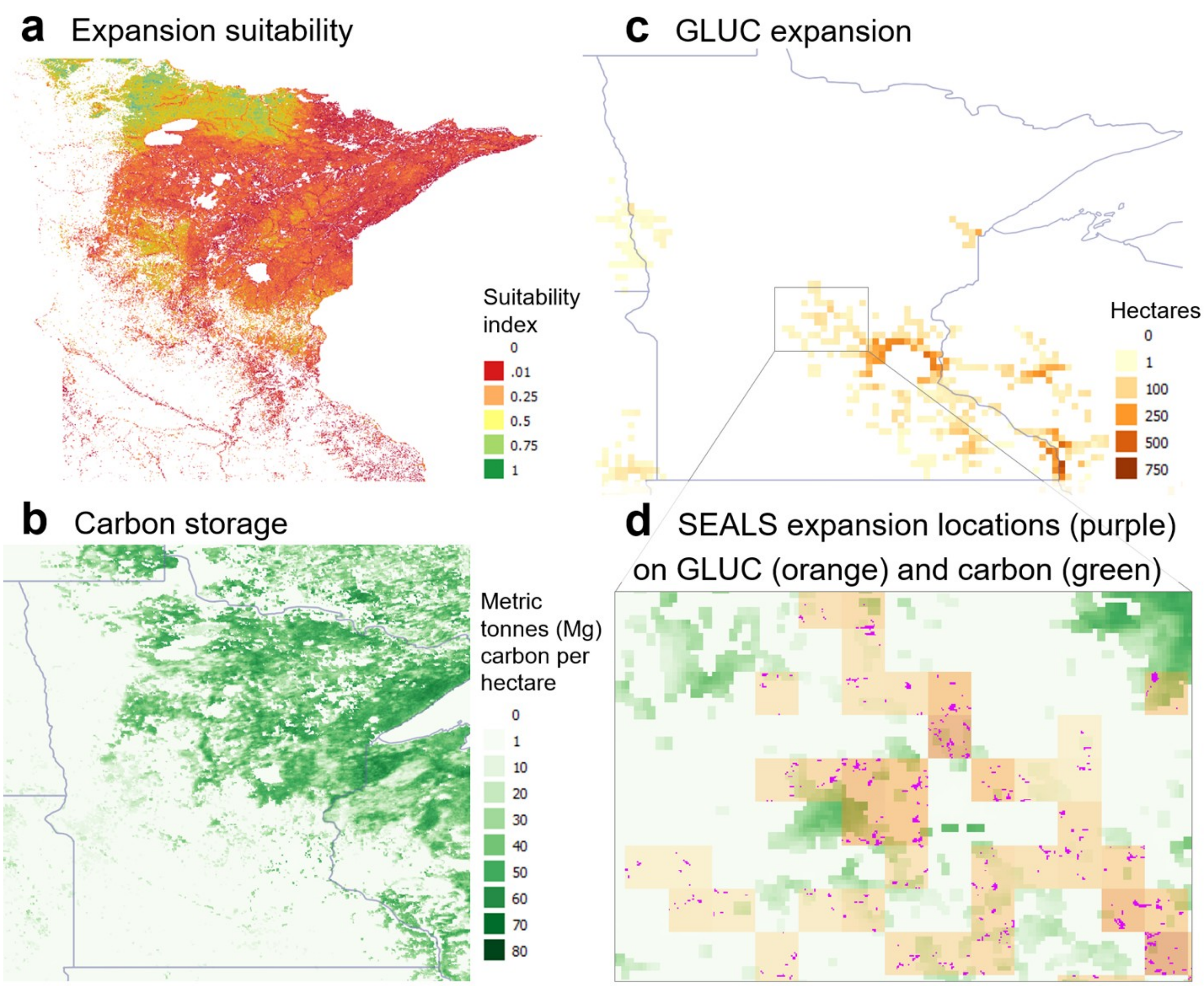

Fig. 4. (a) Suitability for agricultural expansion for maize including adjacency, physical suitability and constraints on cultivation in Minnesota, USA, (b) Mg carbon stock per ha and (c) spatial mapping of GLUC expansion area and (d) SEALS results overlaid on GLUC and carbon results.

3.3 Global spatial patterns

The global spatial patterns of GHG emissions from agricultural expansion for maize are shown in Fig. 5. Expansion may take place across the globe within the known range of maize between 50°N and 45°S[39]. Under the historical yield trend (Scenario 1), expansion encroaches onto some of the tropical climate zones in Central America, Western Africa, and Southern Asia (Fig. 5a). Within the temperate climate zones, maize production under the historical yield trend scenario stretches further to northern and southern boundaries, where crop suitability and yields are lower. Some of the global regions with high carbon stock, including those in Africa, Southern Asia, South America, Eastern Europe, and Central Asia are exposed to maize expansion. Africa, Asia, and Europe (mainly Eastern) combined, contribute 3.4 Gt CO_2e (expansion and intensification) or 81% of the GHG emissions under this scenario. However, under the aggressive yield improvement scenario (Scenario 3), emissions are reduced by 44% in Africa, 60% in Asia, and 76% in Europe (Fig. 5b). Eastern Europe, in particular, shows much higher intensity carbon emissions from agricultural expansion under historical yield trends (Scenario 1, Fig. 5c1) than moderate (Scenario 2, Fig. 5c2) or aggressive yield improvement (Scenario 3, Fig. 5c3) respectively.

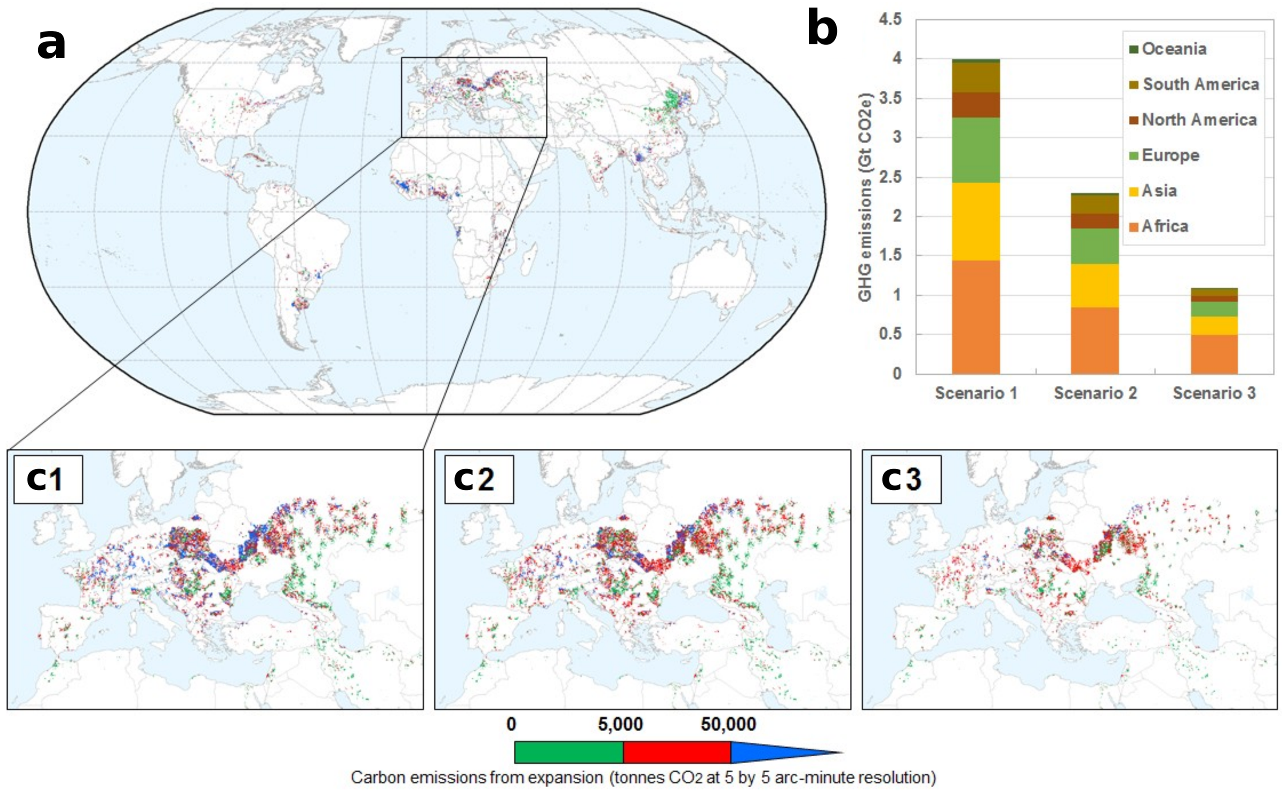

Fig. 5. Aggregate CO_2 emissions from expansion to meet 176 Mt marginal maize demand between 2015 and 2026. (a) Global map of CO_2 emissions from agricultural expansion under Scenario 1; (b) CO_2 emissions at continental level (c) CO_2 emissions in Europe under Scenario 1 (c1): yield improvement following historical trends; Scenario 2 (c2): up to 5% additional yield improvement and Scenario 3 (c3); up to 10% additional yield improvement.

4. Discussion & conclusions

4.1. Implications for GHG emissions modeling

Previous projections and integrated assessment models (IAMs) are generally in good agreement that GHG emissions from global land use change are declining and will diminish to nil in the second half of this century.[4–8] In contrast, our model shows that, for the case of maize, GHG emissions from cropland expansion may rise sharply (contributing ~4.0 Gt CO_2 emissions to global GHG emissions by 2026) to meet the growing maize demand under the current yield improvement trajectory. Furthermore, our findings may underestimate potential GHG emissions since carbon loss from belowground and soil carbon stocks and potential forest edge effects outside of the tropics are excluded.

In addition to the finer spatial resolution employed in our model, two fundamental differences in our modeling approach may explain the contradictory findings. First, Scenario 1 is designed to follow historical yield trends until the maximum potential yield of a given grid-cell (5 by 5 arc-minute resolution) is reached. Historically, improvements in maize yield have been remarkable; globally, a ~50% average yield improvement is observed for maize over the three-decade period between 1980 and 2010[2]. However, there are significant differences among global regions; while average maize yield has doubled in Asia, an increase of only 28% occurred in Africa over the three-decade period[2]. Some regions, like Eastern Europe and West Africa, continue to experience stagnation in yield improvement so that wide yield gaps remain.[9] It is therefore unrealistic to assume a closing of yield gaps across all regions, applying the global average yield improvement trend. Instead, we have used grid-cell by grid-cell yield improvement trends in

Scenario 1.

Second, additional production through intensification becomes increasingly costly as yields approach the maximum potential. As such, a slowing growth in production is expected in regions where near maximum yields are observed. In other words, it is unrealistic to assume that the regions with historically large year-over-year yield improvements will continue the trend indefinitely. In our model, we progressively re-adjust the maximum possible annual yield improvement through intensification based on the previous year's yield gap to simulate the effect of diminishing returns (Section 2.1).

4.2. Agricultural expansion vs. land management emissions

Our results also suggest that additional GHG emissions from intensification in scenarios 2 & 3 are unlikely to negate the avoided CO_2 emissions from agricultural expansion that would otherwise take place. We estimate that in our baseline scenario, marginal N_2O emissions amount to 0.2 Gt CO_2e, accounting for 4.5% of total marginal GHG emissions. Closing the yield gap more expeditiously will increase this contribution to 0.6 - 0.7 Gt CO_2e (Scenarios 3 and 2 respectively) increasing the share of N_2O emissions to 23% - 35% of total marginal GHG emissions. While this offsets some of the GHG reduction obtained from reduced expansion, the total GHG emissions of 1.7 – 3.0 Gt CO_2e for Scenarios 3 and 2 remain significantly lower than the total GHG emissions of the baseline (Scenario 1) of 4.2 Gt CO_2e.

It is notable that Scenario 3 (up to 10% yr^{-1} yield gap closure) leads to somewhat lower N_2O emissions compared to Scenario 2 (up to 5% yr^{-1} yield gap closure), which is counterintuitive. Upon closer inspection, it appears that allowing up to 10% yr^{-1} yield gap closure encourages production from regions with very large yield gaps, whilst using low initial fertilizer inputs, as these areas tend to exhibit higher production per unit nitrogen fertilizer input. As more demand is met by regions with higher N fertilizer efficiency, existing high yield regions with lower N fertilizer efficiency were not selected by the algorithm for production under Scenario 3, leading to a small reduction in global N_2O emissions.

This result confirms that boosting yields is key to reducing future GHG emissions[11], and that accelerating global yield improvement does not necessarily mean higher N_2O emissions if future intensification efforts target the regions with large yield gap and high N fertilizer efficiency.

4.3. Challenges and opportunities in global yield improvement

Our results show that expediting global yield improvement by closing up to 5 – 10% of remaining yield gap per year can substantially reduce the global CO_2 emissions from potential agricultural expansion to 1.1 – 2.3 Gt CO_2 over the 2015 – 2026 period. Understanding the drivers and barriers of yield improvement is therefore crucial for global climate change mitigation. Closing up to 5 – 10% of the yield gap per year, however, is an ambitious goal in many parts of the world. Even though all continents have witnessed significant yield increases over the last decades[18], it is evident that yield change has not been uniform at a finer spatial scale. While yields increased for >70% of harvested areas for maize, 26% and 3% of harvested areas experienced yield stagnation and yield collapse, respectively[9]. Furthermore, significant disparity in yields persists among different regions of the globe: in 2015, the average maize yield was over 10 t ha^{-1} in North America, but it was only ~2 t ha^{-1} in Africa[18], despite estimations that Africa can potentially produce ~4 t of maize per ha[40,41]. Similarly, significant yield gaps persist in Eastern Europe, Central America, and South Eastern Asia.

Various intangible barriers to yield improvement have been reported including the lack of access to information and capital, limitations in human resources, and inadequate incentive structures associated with farmland tenure arrangements[42,43]. In many cases, the barriers to yield gap closure need to be understood from a local context. For example, where fragile soils are prevalent, implementation of specific soil conservation strategies and improved management of water (as opposed to higher fertilizer inputs) are likely needed to realize yield improvements[44]. Local knowledge or incentives for such strategies may be varied or lacking. Other barriers include the limited access to high yielding varieties which can deliver yield expectations even under marginal conditions[44].

Sustainable intensification[11] would need a combination of complementary strategies[45], including regulatory interventions[46,47], market instruments[48], and producer behavioral changes[49,50].

4.4. Needs for multi-layered, GHG mitigation efforts

Limiting global mean temperature rise from pre-industrial levels to well below 2°C requires achieving net zero GHG emissions by the second half of the century[51-53]. Our study indicates that crop land expansion, demonstrated here focusing on maize demand projections in the coming decade, may pose a challenge to achieving this goal. There is an urgent need to close the global yield gap, through locally relevant interventions targeted for regions with high yield gaps and fertilizer deficit, to prevent large-scale GHG emissions from maize expansion. Given the potential local challenges associated with accelerating yield gap closure, however, other complementary strategies should be pursued in parallel to reduce demand or redirect expansion away from high carbon stock areas. Literature suggests dietary changes and demand management[49,54], market instruments[55,56], regulatory interventions[46,47], voluntary pledges and agreements, and various combinations thereof[45] as potential strategies. However, many of these strategies are likely to generate consequences which reach far beyond the production of a single crop. Although not demonstrated here, our modeling approach could be further developed to accommodate simultaneous modeling of multiple crops, thereby facilitating consideration of these broader supply and demand changes and land use competition between crops.

4.5. Future research

Future research should explore uncertainties and stochastic modeling approaches as well as the effect of climate change on yield at fine spatial resolution. Alternative strategies to fertilizer use for yield improvement including irrigation, improved crop management, mechanization, and the use of better cultivar and agrochemicals could be more explicitly incorporated into yield projection models. Examining the potential of these land management approaches individually and in combination at a regional level would help understand the regional differences in yield improvement trends and inform strategies to overcome yield stagnation. Finally, in this paper, we have examined maize supply and demand until 2026; future research could extend modeling for simultaneous consideration of multiple crops over extended time periods.

Data availability

All data generated or analyzed during this study are freely available at https://github.com/VitalMetrics-IERS/GLUC-Model.

Code availability

The GLUC and SEALS model codes are freely available at https://github.com/VitalMetrics-IERS/GLUC-Model.

References

1. Foley, J. A. *et al.* Global consequences of land use. *Science* **309**, 570–574 (2005).

2. FAO. *FAO STAT*. (2018).

3. Houghton, R. A. *et al.* Carbon emissions from land use and land-cover change. *Biogeosciences* **9**, 5125–5142 (2012).

4. Smith, P. *et al.* Agriculture, Forestry and Other Land Use (AFOLU). in *Climate Change 2014: Mitigation of Climate Change. Contribution of Working Group III to the Fifth Assessment Report of the Intergovernmental Panel on Climate Change [Edenhofer, O., R. Pichs-Madruga, Y. Sokona, E. Farahani, S. Kadner, K. Seyboth, A. Adler, I. Baum, S. Brunner, P. Eickemeier, B. Kriemann, J. Savolainen, S. Schlömer, C. von Stechow, T. Zwickel and J. Minx (eds.)]* (Cambridge University Press, 2014).

5. Kriegler, E. *et al.* The role of technology for achieving climate policy objectives: overview of the EMF 27 study on global technology and climate policy strategies. *Clim. Change* **123**, 353–367 (2014).

6. Popp, A. *et al.* Land-use protection for climate change mitigation. *Nat. Clim. Change* **4**, 1095–1098 (2014).

7. Tubiello, F. N. *et al.* Agriculture, forestry and other land use emissions by sources and removals by sinks. *Stat. Div. Food Agric. Organ. Rome* (2014).

8. Tubiello, F. N. *et al.* The contribution of agriculture, forestry and other land use activities to global warming, 1990–2012. *Glob. Change Biol.* **21**, 2655–2660 (2015).

9. Ray, D. K., Ramankutty, N., Mueller, N. D., West, P. C. & Foley, J. A. Recent patterns of crop yield growth and stagnation. *Nat. Commun.* **3**, 1293 (2012).

10. Ray, D. K., Mueller, N. D., West, P. C. & Foley, J. A. Yield Trends Are Insufficient to Double Global Crop Production by 2050. *PLOS ONE* **8**, e66428 (2013).

11. Tilman, D., Balzer, C., Hill, J. & Befort, B. L. Global food demand and the sustainable intensification of agriculture. *Proc. Natl. Acad. Sci.* **108**, 20260–20264 (2011).

12. FAO. *FAO Cereal Supply and Demand Brief, World Food Situation*. http://www.fao.org/worldfoodsituation/csdb/en/ (2018).

13. USDA-FAS. *Grains: Production, Supply and Distribution*. https://apps.fas.usda.gov/psdonline/app/index.html#/app/downloads (2018).

14. Smith, S. *et al.* Maize. *Yield Gains Major US Field Crops* 125–172 (2014).

15. Assefa, Y. *et al.* A new insight into corn yield: trends from 1987 through 2015. *Crop Sci.* **57**, 2799–2811 (2017).

16. Loarie, S., Lobell, D., Asner, G., Mu, Q. & Field, C. Direct impacts on local climate of sugar-cane expansion in Brazil. *Nat. Clim. Change* **1**, 105–109 (2011).

17. Tollenaar, M., Fridgen, J., Tyagi, P., Stackhouse Jr, P. W. & Kumudini, S. The contribution of solar brightening to the US maize yield trend. *Nat. Clim. Change* **7**, 275 (2017).

18. FAO. *OECD-FAO Agricultural Outlook 2018-2027*. (2018).

19. Mueller, N. D. *et al.* Closing yield gaps through nutrient and water management. *Nature* **490**, 254–257 (2012).

20. Chaplin-Kramer, R. *et al.* Spatial patterns of agricultural expansion determine impacts on biodiversity and carbon storage. *Proc. Natl. Acad. Sci.* **112**, 7402–7407 (2015).

21. Chaplin-Kramer, R. *et al.* Life cycle assessment needs predictive spatial modelling for biodiversity and ecosystem services. *Nat. Commun.* **8**, ncomms15065 (2017).

22. Ermolieva, T. Y. *et al.* Systems analysis of robust strategic decisions to plan secure food, energy, and water provision based on the stochastic GLOBIOM model. *Cybern. Syst. Anal.* **51**, 125–133 (2015).

23. Valin, H. *et al.* Description of the GLOBIOM (IIASA) model and comparison with the MIRAGE-BioF (IFPRI) model. *Crops* **8**, (2013).

24. Wise, M., Dooley, J., Luckow, P., Calvin, K. & Kyle, P. Agriculture, land use, energy and carbon emission impacts of global biofuel mandates to mid-century. *Appl. Energy* **114**, 763–773 (2014).

25. Lotze-Campen, H. *et al.* Food demand, productivity growth and the spatial distribution of land and water use: a global modeling approach. *Agric. Econ.* **39**, 325–338 (2008).

26. Dietrich, J. P., Schmitz, C., Lotze-Campen, H., Popp, A. & Müller, C. Forecasting technological change in agriculture—An endogenous implementation in a global land use model. *Technol. Forecast. Soc. Change* **81**, 236–249 (2014).

27. Asner, G. P. *et al.* High-resolution forest carbon stocks and emissions in the Amazon. *Proc. Natl. Acad. Sci.* **107**, 16738–16742 (2010).

28. Chaplin-Kramer, R. *et al.* Degradation in carbon stocks near tropical forest edges. *Nat. Commun.* **6**, 10158 (2015).

29. Duchin, F. & Levine, S. H. Sectors May Use Multiple Technologies Simultaneously: The Rectangular Choice-Of-Technology Model With Binding Factor Constraints. *Econ. Syst. Res.* **23**, 281–302 (2011).

30. Kätelhön, A., von der Assen, N., Suh, S., Jung, J. & Bardow, A. Industry-Cost-Curve Approach for Modeling the Environmental Impact of Introducing New Technologies in Life Cycle Assessment. *Environ. Sci. Technol.* **49**, 7543–7551 (2015).

31. Kätelhön, A., Bardow, A. & Suh, S. Stochastic Technology Choice Model for Consequential Life Cycle Assessment. *Environ. Sci. Technol.* **in press**, (2016).

32. Bontemps, S. *et al.* Consistent global land cover maps for climate modelling communities: current achievements of the ESA's land cover CCI. in *Proceedings of the ESA Living Planet Symposium* 9–13 (2013).

33. Hengl, T. *et al.* SoilGrids250m: Global gridded soil information based on machine learning. *PLoS One* **12**, e0169748 (2017).

34. Defourny, P. *et al.* The Land Cover component of the ESA Climate Change Initiative. Extending the series of global land cover maps to 2015 with PROBA-V: current achievements. in (2016).

35. Santoro, M. *GlobBiomass - global datasets of forest biomass*. (PANGAEA, 2018). doi:10.1594/PANGAEA.894711.

36. IPCC. *Guidelines for national greenhouse gas inventories. Prepared by the National Greenhouse Gas Inventories Programme*. (2006).

37. Ruesch, A. & Gibbs, H. K. New IPCC Tier-1 global biomass carbon map for the year 2000. (2008).

38. De Klein, C. *et al.* N2O emissions from managed soils, and CO2 emissions from lime and urea application. *IPCC Guidel. Natl. Greenh. Gas Invent. Prep. Natl. Greenh. Gas Invent. Programme* **4**, 1–54 (2006).

39. Leff, B., Ramankutty, N. & Foley, J. A. Geographic distribution of major crops across the world. *Glob. Biogeochem. Cycles* **18**, (2004).

40. Ramankutty, N., Evan, A. T., Monfreda, C. & Foley, J. A. Farming the planet: 1. Geographic distribution of global agricultural lands in the year 2000. *gbc* **22**, (2008).

41. Monfreda, C., Ramankutty, N. & Foley, J. A. Farming the planet: 2. Geographic distribution of crop areas, yields, physiological types, and net primary production in the year 2000. *Glob. Biogeochem. Cycles* **22**, (2008).

42. Obidike, N. A. Rural farmers problems accessing agricultural information: a case study of Nsukka local government area of Enugu State, Nigeria. *Libr. Philos. Pract.* (2011).

43. Feder, G., Just, R. E. & Zilberman, D. Adoption of agricultural innovations in developing countries: A survey. *Econ. Dev. Cult. Change* **33**, 255–298 (1985).

44. Meyer, R. Low-input intensification in agriculture chances for small-scale farmers in developing countries. *Gaia-Ecol. Perspect. Sci. Soc.* **19**, 263–268 (2010).

45. Smith, P. *et al.* How much land-based greenhouse gas mitigation can be achieved without compromising food security and environmental goals? *Glob. Change Biol.* **19**, 2285–2302 (2013).

46. Busch, J. *et al.* Reductions in emissions from deforestation from Indonesia’s moratorium on new oil palm, timber, and logging concessions. *Proc. Natl. Acad. Sci.* **112**, 1328–1333 (2015).

47. Kastens, J. H., Brown, J. C., Coutinho, A. C., Bishop, C. R. & Esquerdo, J. C. D. Soy moratorium impacts on soybean and deforestation dynamics in Mato Grosso, Brazil. *PloS One* **12**, e0176168 (2017).

48. Cooper, R. N. *et al. Global Carbon Pricing: The Path to Climate Cooperation*. (MIT Press, 2017).

49. Bajželj, B. *et al.* Importance of food-demand management for climate mitigation. *Nat. Clim. Change* **4**, 924–929 (2014).

50. Hedenus, F., Wirsenius, S. & Johansson, D. J. A. The importance of reduced meat and dairy consumption for meeting stringent climate change targets. *Clim. Change* **124**, 79–91 (2014).

51. IPCC. Climate Change 2014: Mitigation of Climate Change - Intergovernmental Panel on Climate Change. (2014).

52. UNFCCC. *Adoption of the Paris Agreement*. http://unfccc.int/resource/docs/2015/cop21/eng/l09.pdf (2015).

53. Schleussner, C.-F. *et al.* Science and policy characteristics of the Paris Agreement temperature goal. *Nat. Clim. Change* **6**, 827–835 (2016).

54. Springmann, M., Godfray, H. C. J., Rayner, M. & Scarborough, P. Analysis and valuation of the health and climate change cobenefits of dietary change. *Proc. Natl. Acad. Sci.* 201523119 (2016) doi:10.1073/pnas.1523119113.

55. Alix-Garcia, J. & Wolff, H. Payment for Ecosystem Services from Forests. *Annu. Rev. Resour. Econ.* **6**, 361–380 (2014).

56. World Bank. *State and Trends of Carbon Pricing 2018*. https://openknowledge.worldbank.org/handle/10986/29687 (2018).